

doi:10.15199/48.2022.05.10

## Rotating polarization microstrip antenna for DSRC system

**Streszczenie.** W pracy przedstawiono zaprojektowaną i wykonaną antenę o polaryzacji wirującej z przeznaczeniem do systemu DSRC. Antena wykonana w technologii drukowanej. Zaprezentowano i omówiono otrzymane charakterystyki promieniowania anteny systemie 3D oraz jej dopasowanie. **Antena mikropaskowa o polaryzacji wirującej przeznaczona do systemu DSRC**

**Abstract.** The paper presents a designed and manufactured antenna with rotating polarization intended for the DSRC system. The antenna is made in printed technology. The obtained antenna radiation characteristics in the 3D system and its matching were presented and discussed.

**Słowa kluczowe:** Charakterystyka anteny, system DSRC, antena mikropaskowa, polaryzacja wirująca.

**Keywords:** Antenna characteristics, DSRC systems, microstrip antenna, rotating polarization

### Introduction

The antenna has become one of the most difficult challenges in the design of wireless communication systems in portable devices [1]. Due to the limited space available for an antenna, shrinkage of conventional antennas can lead to performance degradation and complex mechanical assembly. The technology of microstrip antennas makes it possible to design an antenna with smaller dimensions at lower costs with better performance parameters both at the antenna and system level [2, 3]. Various implementations of microstrip antennas have been described and demonstrated [4, 5]. In this study, a rotating polarization microstrip antenna for the DSRC system was tested and applied

At a time when rush and time optimization to the highest extent have become the most important challenges for humanity, the RFID system is a very important part of the technological word. The RFID [6], system is based on the ISM band – Industrial, Scientific, Medical, it is an unlicensed band, the frequencies of which are used by wireless system such as Bluetooth, WiFi [7].

- Low frequency (LF) – tags operate at 125 kHz to 134,2 kHz,
- High frequency (HF) – tags work at 13,56 MHz,
- Ultra high frequency (UHF) – tags work at 433 MHz and 860-960 MHz,
- Microwaves tags work on the frequencies of 2.4 GHz and 5.9 GHz, are available as passive, semi-passive and active, their size is the smallest of all, but have the largest range.

For passive tags, it is about 5m, half-passive tags are 30m and active tags are over 100m. Due to shorter wavelength, cooperation with metal objects is easier, in addition, anti-collision protocols are available, and due to wider frequency range more channels are used, all of which contribute to better tag reading. Due to low number of regulations and standards, this spectrum has a lot of freedom and scope.

One of the many paths in which RFID development is heading is the Dedicated Short-Range Communications System. The best known way of usage of DSRC is viaToll, i.e. the automatic toll collection system on Polish and European motorways.

DSRC system - enables quick communication between vehicles and road points or other vehicles while in motion [7]. Due to the high-speed data transfer between vehicles, it can be used in rapid road collision warning systems, saving thousands of lives. Vehicles equipped with the DSRC system can send information to other vehicles about their location, acceleration and speed and compare it several times per second. After sending and receiving such signals,

it is possible to compare the data and predict the trajectory of other road users, giving the opportunity to be warned about a possible collision. Another possibility of using it is communication with roadside units that send a signal about possible difficulties, bad weather conditions or about the risk on the road. In addition to being able to react quickly, it can be used for other purposes, such as electronic toll collection, parking or refuelling.

The frequency on which the system operates is internationally standardized to 5.9 GHz with a 75 MHz band (5.875-5.950 GHz). The communication range is several hundred meters. Wireless car communication can become a way to increase road safety, prevent collisions and facilitate traffic. In order to achieve this there is a need for common interoperability standard. Standards are being developed and implemented, including the IEEE 802.11p standard – a subgroup of IEEE 802 standards that describe the physical layer and the MAC sub-layer for wireless connectivity in the vehicle environment [6]. It is an extension of the IEEE 802.11 standard, which is the basic for the WiFi network required to operate the Intelligent Transport System (ITS). ITS involves data exchange between vehicles or vehicle and road infrastructure in the licensed band for ITS of 5.9 GHz. Referring to the requirements listed in ITS, we can define that the antennas intended for use in this system must have, among other, a wide radiation pattern, rotating polarization, relatively small geometric dimension and good match between antenna and cable impedance.

Currently, one of the most innovative fields of antenna technology is the field of microstrip antennas [13, 18]. Microstrip antennas have many interesting features, such as:

- accurate representation on the surface,
- low manufacturing cost,
- high repeatability of performance,
- insignificant volume,
- operating frequency masking,
- simplicity of production, provided that relatively advanced technologies are used,
- flat shape and low weight allow the use of antennas on a dielectric basis on fast-flying objects without fear of deteriorating their aerodynamic properties.

However, the dielectric substrate used favors the excitation of surface waves, which, propagating along the dielectric plane, interfere with the normal operation of the antenna [8]. Other disadvantages of microstrip antennas are:

- narrow bandwidth,
- limited power load.

These antennas allow for the miniaturization of the antenna system, thus increasing its density. This causes the occurrence of mutual couplings changing the field distributions on aperture antennas and the current distributions in linear antennas. This state of affairs, in turn, changes the spatial characteristics of antenna radiation and their input impedance.

The article presents a designed microstrip antenna with rotating polarization and powered by a single point. The antenna has bevelled antenna horns, which disrupts the distribution of currents on the antenna, and thus the possibility of generating two modes necessary to obtain rotating polarization. Unfortunately, such a construction did not meet the requirements as the required polarization was not achieved.

Therefore, additional indentations were made in the side edges in order to further disturb the current distribution on the antenna. Only this procedure ensured the required polarization, which after this procedure is. The indentations at the power line allowed to obtain the required input impedance. The resulting impedance is 50 Ω. Then the results of measurements of the characteristics of these antennas are presented. High compliance has been achieved.

### Analysis of antenna radiation on a dielectric substrate with rotating polarization

Rotating polarization can be resolved into a pair of oscillation of the same amplitude but with a phase shifted by exactly 90° or 270°, so that the oscillation corresponds to a movement in a circle or an ellipse. Depending on the shift, we can talk about right-handed or left-handed circular polarization, respectively, resulting from the rotation of the vector to the right or left. It follows that to obtain a rotating polarization, the following conditions must be met:

Create two mutually perpendicular fields in the antenna  
Obtain the delay of one component of field by π/2 or K π/2, where K = (2n-1), n-natural number,  
Put both components together.

Obtaining rotating polarization in microstrip antennas with a rectangular element powered at one point is possible in several ways [9]:

- Connect the line to the power supply in the corner of the rectangle
- Cut off the two opposite corners of the radiating element
- Cut a rectangle in the radiating element at an angle of 45° on the diagonal of the rectangle
- Add symmetrical rectangles to the sides of the radiating element
- Create two symmetrical rectangles on the sides of the rectangular radiating element,
- Cut two squares at opposite corners of the radiator

Most practical designs of spinning polarization microstrip antennas try to commit complexity of construction related to excitation at two points. It is related to the influence of power lines on radiation of antennas of this type. Therefore, the excitation of two perpendicular types of vibrations is performed at one point - determined in a way that the amplitudes of the excited fields are the same [10, 11]. A rotating polarization antenna can be represented as a system of three main parts connected in a following cascade:

- power supply networks, transition from concentric to strip line,
- matching system,
- an antenna element

The properties of each of these elements can be described by the parameters of the four-terminal network. And describe the whole system in the form of a scattering matrix:

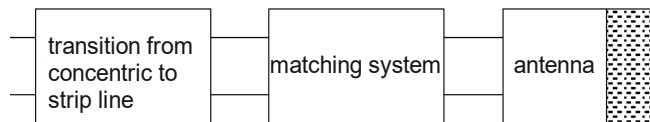


Fig. 1 Model of antenna with rotating polarization in the form of a cascade of quadrants

The antenna's scattering matrix can be expressed as:

$$(1) \quad \begin{bmatrix} b_1^A \\ b_2^A \\ b_3^A \\ b_4^A \end{bmatrix} = \begin{bmatrix} S_{11}^A & S_{12}^A \\ S_{21}^A & S_{22}^A \\ S_{31}^A & S_{32}^A \\ S_{41}^A & S_{42}^A \end{bmatrix} \begin{bmatrix} a_1^A \\ a_2^A \end{bmatrix}$$

Each of the waves fed to the system has a separate transmission line. The structure has different properties for each wave

$a_1^A, a_2^A$  incident waves on the entrance;

$b_1^A, b_2^A$  waves reflected towards the main feeding line;

$b_3^A, b_4^A$  waves reflected towards free space;

$S_{31}^A, S_{32}^A, S_{42}^A, S_{42}^A$ , describe antenna radiation.

The components of the radiation field → are:

$$(2) \quad b_3^A = S_{31}^A a_1^A + S_{32}^A a_2^A \rightarrow b_3^A \rightarrow E_\theta \rightarrow (E_{X1}); E_{Y1}$$

$$(3) \quad b_4^A = S_{41}^A a_1^A + S_{42}^A a_2^A \rightarrow b_4^A \rightarrow E_\phi \rightarrow (E_{X2}); E_{Y2}$$

The parameter characterizing the ellipticity is the axial ratio:

$$(4) \quad AR = 10 \log \frac{|k^2| + 1 + [|k|^4 + 1 + 2|k|^2 \cos(2\Delta\psi)]^{0.5}}{|k^2| + 1 - [|k|^4 + 1 + 2|k|^2 \cos(2\Delta\psi)]^{0.5}}$$

where:

$$(5) \quad k = \frac{E_\theta}{E_\phi} = \left| \frac{E_\theta}{E_\phi} \right| \exp(i\Delta\psi) = \frac{b_3^A}{b_4^A} = \frac{S_{31}^A a_1^A + S_{32}^A a_2^A}{S_{41}^A a_1^A + S_{42}^A a_2^A}$$

With the assumed ellipticity AR, we can determine the circular area in the complex plane for the permissible ratio  $E_\theta/E_\phi$ . The figure shows one of the two possible areas that meet the given elliptical condition. The position of the end of the vector  $E_\theta$  on the circle corresponds to the determined ellipticity value [8]. The antenna, which is excited by two mutually perpendicular fields, produces a rotating polarization.

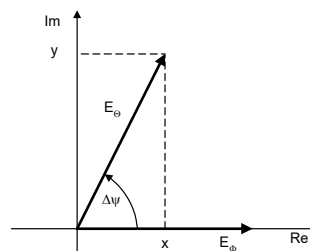


Fig. 2 Area with a given ellipticity coefficient

Presented logic leads to the determination of the parameters of the polarization ellipse of the radiated field under given excitation conditions. It allows to predict the shape of the polarization ellipse depending on the mutual relations between the waves incident on the antenna entrance gate.

### Antenna design in CST microwave studio environment

Along with development of theories and techniques of microstrip antennas we can use different ways of modelling the antennas [12] most popular ones are:

- transmission model
- cavity model,
- current net model,
- full wave model.

Selection of a proper analytic method depends on model of designed or analysed antenna [13]. In microstrip antennas we need to pay attention to connection of field and circuit aspects which results in more complex methods used to analyse them. Selection of proper parameters of antenna is the most important issue to be taken into account while designing of the antenna [14]. Nowadays designing of antennas is done in two steps. In the first phase basic geometrical dimensions: length (L) and width (W) are selected. Transmission line model is being used to determine those values. One of the most important parameters are geometrical length and width of radiator. Their values have been defined by usage of transmission line model based on following relations:

$$(6) \quad \epsilon_{re} = \frac{\epsilon_r + 1}{2} + \frac{\epsilon_r - 1}{2} \left(1 + 12 \frac{h}{W}\right)^{-1/2}$$

$\epsilon_{re}$  - effective dielectric constant

$$(7) \quad L = \frac{c}{2f_r \sqrt{\epsilon_{re}}} - 2\Delta L$$

$$(8) \quad W = \frac{c}{2f_0 \sqrt{\frac{\epsilon_r + 1}{2}}}$$

In order to improve the calculation of the parameters of the microstrip antenna, a program was prepared in the MATLAB R2016b environment. On the other hand, the CST (Computer Simulation Technology) environment based on FDTD [15, 16] was used to optimize the dimensions of the antenna elements. It was done manually using the built-in Optimizer function, the dimensions of the excitation and radiating elements were optimized. Then, the SWR, S11, current distribution and radiation pattern of the antenna designed in this way were calculated.

The most important quantities describing the designed antenna are width W and length L of the radiator. The length of the radiator is a critical parameter as it determines the resonant frequency of the antenna. The width, on the other hand, affects the input impedance and the bandwidth of the operation, its increase results in an increase in the radiated power and radiation efficiency. It is assumed that the ratio of width to length of the radiator should be  $1 \leq W/L \leq 2$ . Then, using the long line model [13,], the width (W) and length (L) were determined.

Fr-4 laminate with a copper thickness for the screen and a radiating patch  $h = 35 \mu\text{m}$  and dielectric thickness  $h_d = 1.56 \text{ mm}$ , relative electric permeability  $\epsilon_r = 4.3$  and loss angle  $\text{tg}\delta = 0.025$  has been used. The frequency used in the DSRC system is  $f = 5.9 \text{ GHz}$  and band  $B = 75 \text{ MHz}$ . Based on these data, the width (W) and length (L) of the radiating element in the antenna were determined using the slit model. The results obtained are accordingly  $W = 15.61 \text{ mm}$  and  $L = 11.69 \text{ mm}$ . The dimensions of the screen and the dielectric are the same and equal to twice the length and width of the radiating patch. That is,  $W_g = 31.22 \text{ mm}$  and  $L_g = 23.38 \text{ mm}$ . As previously mentioned, the antenna in the DSRC system should have a rotating polarization and a broad radiation pattern. In order to obtain the rotating polarization, two opposite antenna corners were cut. The frequency range of the designed antenna is the lower frequency of 4 GHz, and the maximum 7 GHz. The antenna designed [17, 18, 19], in the CST software had the parameters listed in Table 1, and a power line with a width of  $W_f = 3.058 \text{ mm}$ , connector impedance is 50  $\Omega$ .

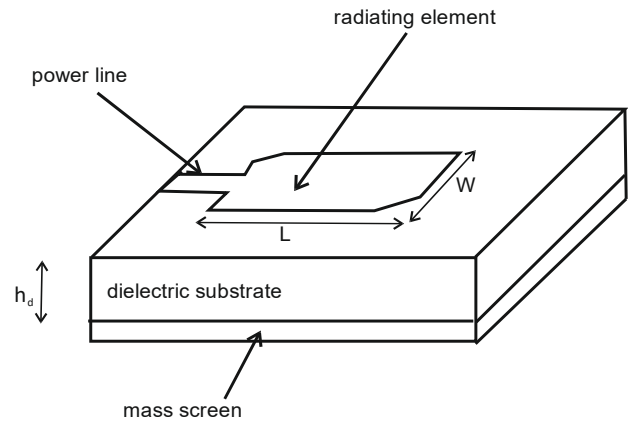


Fig. 3. Basic structure of a microstrip antenna with a description of its dimensions [2]

This width was calculated thanks to the built-in input impedance calculator in the program. The opposite truncated corners length is  $W_r = 2.6 \text{ mm}$ .

$$(9) \quad W_r = \frac{W}{4}$$

In order to optimize the antenna, several changes were made to its dimensions:

- Notches in the radiating patch
- Cut-outs at the feed line
- Reduced dielectric dimensions

The changes resulted in obtaining the appropriate resonance frequency, increasing the antenna's efficiency.

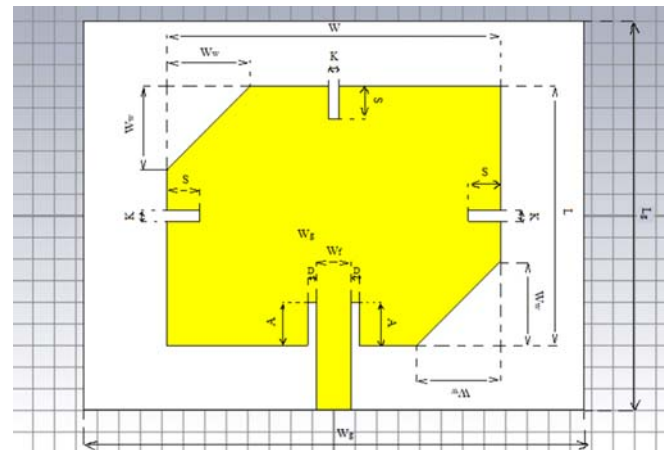


Fig. 4. Optimized circular polarization antenna

Table 1. Optimized antenna dimensions

Dimension	Value [mm]
The width of the radiating patch W	15,5
The length of the radiating patch L.	11,97
Feed line width $W_f$	1,8
Cutout width at power line D	0,4
Cutout Length at Supply Line A.	2
Corner notch length $W_w$	3,875
The length of the cut-out in the sides of the radiating batten S.	1,5
Width of the cutout on the sides of the radiating batten K	0,5
Dielectric width $A_{cc}$	23,25
Dielectric length $L_g$	17,955

Feed line width  $W_f$  cut-out width at feed line D. Cut-out Length at Supply Line A.  $W_w$  corner notch length The length of the cut-out in the sides of the radiating patch S.

Unfortunately, the designed antenna obtained a very low rotating polarization. The obtained polarization index is AR-28.94 dB. Therefore, one of the above-mentioned solutions for obtaining the rotating polarization was additionally used, i.e. the introduction of symmetrical rectangular cuts on the sides of the radiating element. These notches are designed to disturb the distribution of currents in the antenna aperture and excite two orthogonal modes, and thus the rotating polarization

**Simulations**

After completing the project, a series of simulations were carried out to determine the simulation of electrical parameters and radiation characteristics of the antenna. The advantage of the CST Microwave Studio environment is the high convergence of the simulation results with the later results obtained through laboratory tests, assuming high accuracy of the antenna [17]. Unfortunately, the entered data obtained from the transmission line method did not provide the required parameters, especially the axial ratio of the two orthogonal components of the electromagnetic field. In order to improve this ratio, indentations were introduced both at the feed line and on the side edges of the antenna. These modifications made it possible to obtain the required parameters. Figures 5 to 9 show the obtained simulation results of the final antenna model [16.]. The value of the antenna gain obtained by the simulation is 2.08 dB. Considering the fact that the antenna has a radiation pattern similar to a half-wave dipole, the obtained value is satisfactory.

The following results have been obtained:

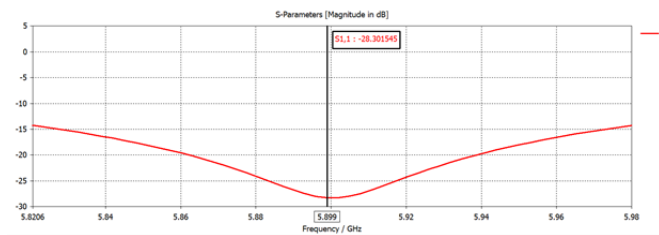


Fig. 5 Characteristics of the S<sub>11</sub> parameter for a simulated antenna

The characteristic presented in Figure 5 shows the S<sub>11</sub> parameter for the designed antenna. It is -28.3 dB for the value f<sub>r</sub> = 5.899 GHz. This value is an very good result. Additionally, the frequency at which S<sub>11</sub> is lowest is the desired frequency at which the antenna is to operate. For the antenna designed SWR for the frequency 5.899 GHz it was 1.08 which means that the antenna is well matched, as the result is close to 1

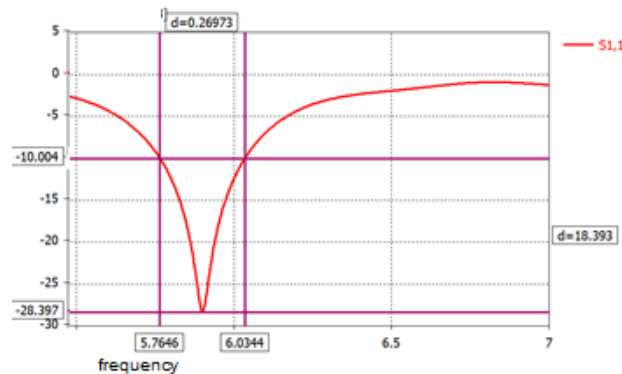


Fig.6 Bandwidth antenna

The resonant frequency f<sub>r</sub> is the frequency value for which the antenna works most efficiently. For the designed antenna the frequency is f<sub>r</sub> = 5.899 GHz. The value that was

desired for the project was 5.9 GHz, which is a very good result.

Figure 6 shows the operating range of the designed antenna. The band is 269 MHz. Bandwidth is wider than expected.

The impedance represents the antenna load on the generator. It was set to 50 Ω. The characteristics presented below show the real part (Fig. 7a) and the imaginary part (Fig. 7b) of the antenna. The resistance at the resonant frequency is 53.69 Ω and the imaginary part is

-1.57 Ω. The above characteristic shows the antenna impedance of 53.71 Ω. The result is good, the value that assumed when designing the antenna was 50 Ω

It can be depicted in various planes. The expected result of the radiation pattern was energy radiation over a wide range of angles. However, due to the screen on the rear of the antenna, the signal is attenuated. Despite this, the obtained effect is satisfactory. Below is the representation of the characteristics in three planes in 3D.

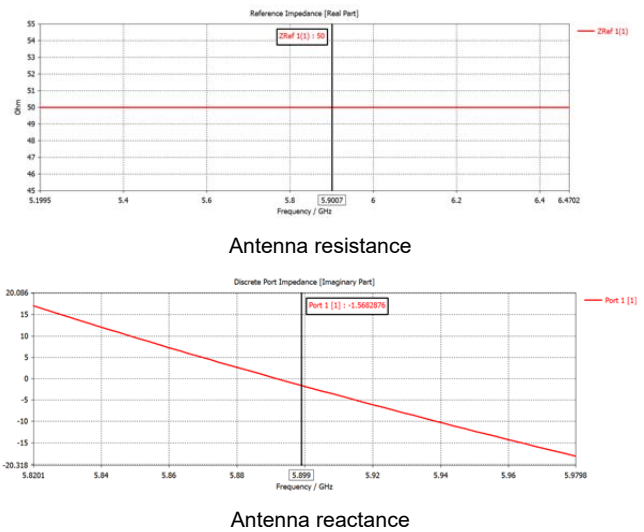
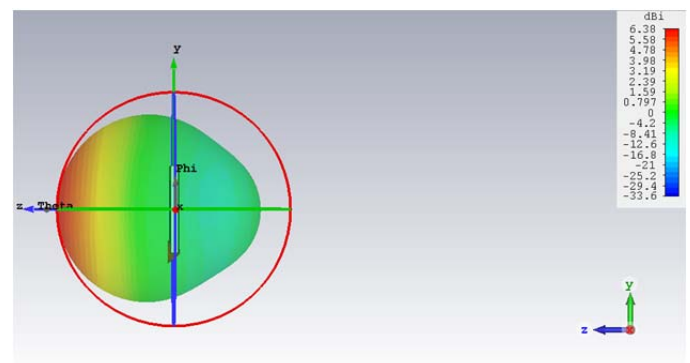


Fig. 7 Antenna impedance

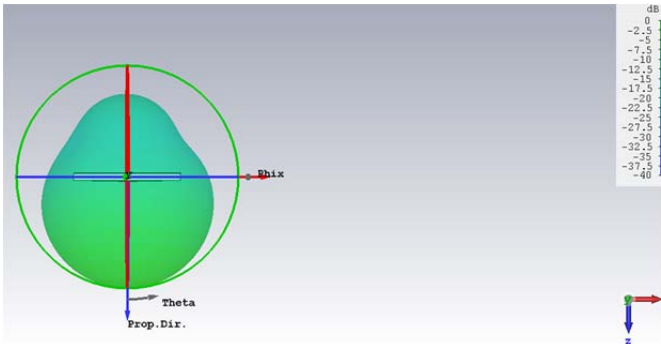
The antenna polarization can be determined by simulating the radiation pattern. The goal was to achieved circular polarization.

The antenna polarization can be determined by simulating the radiation pattern..

The axial ratio is the ratio of the two orthogonal components of the electric field. For circular polarization, the field consists of two orthogonal components of equal amplitude and 90° difference. For circular polarization, the ratio should be 1.



Antenna side view



Top view of the antenna

Fig.8 Antenna radiation pattern in 3D imaging

The simulations show that the maximum AR <10 dB, which means that the obtained polarization is an elliptical rotating polarization. The circular polarization effect was not obtained, but in our case AR is satisfactory

### Examination of the designed model

The figure shows a fabricated antenna model. The antenna shape was cut with a plating engraving plotter. Due to the lack of precision i.e. during cutting, some operations required the operator's precision, e.g. the depth of the dielectric incision, the dimensions of the plate may not coincide perfectly with the values from the simulation environment, which may distort the results.

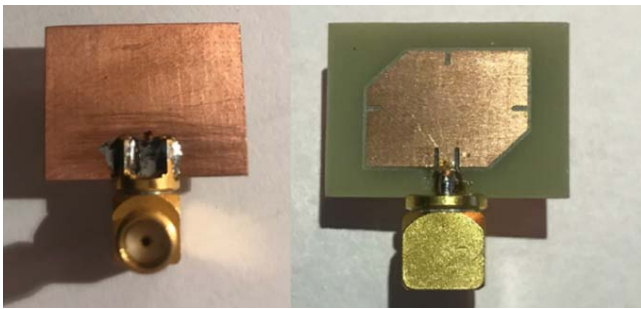


Fig.9 Fabricated antenna model

The first series of measurements took place in an anechoic chamber.

After checking the condition of the far zone and obtaining positive results measurements were carried out. The width of the main lobe for both the computer simulation and the obtained measurement results is almost the same. On the other hand, the difference is in the back lobe, it is greater for the measurements carried out.

. As a result, the main beam width is different here and amounts to 95 degrees. In order to compare the simulation results and measurements made for the physical antenna model, three parameters were tested: – Parameter  $S_{11}$  – SWR – Antenna impedance

The reflectance characteristic for the tested antenna looks like in figure 10. The resonant frequency for the made antenna is 5.907 GHz.  $S_{11} = -10.87$  dB for the frequency  $f_r$ . The loss of antenna efficiency can be caused by many factors, including:

- Inaccurate dimensions of the antenna
- Higher connector impedance
- Poor connector quality

Due to the imperfect representation of the simulated antenna, the drop can also be observed in the standing wave ratio. Antenna matching is less accurate.

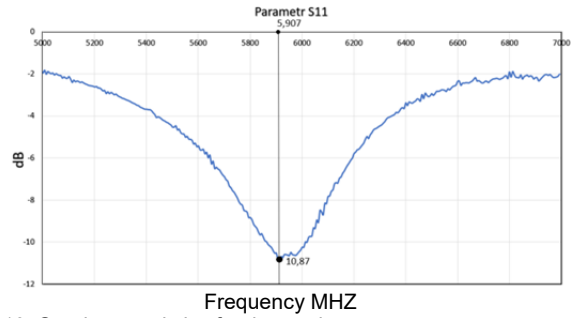


Fig. 10.  $S_{11}$  characteristics for the made antenna

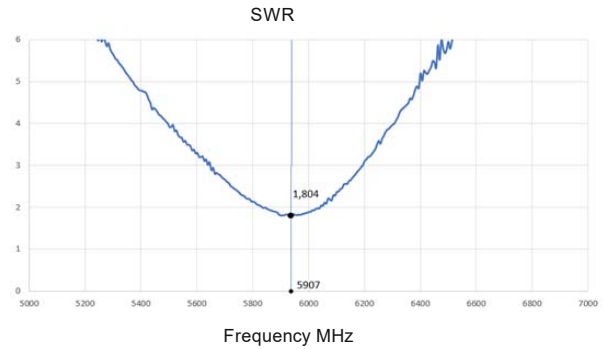


Fig. 11. SWR characteristics for the antenna made

The reason for the deterioration may be a change in the feeding line width, as well as the joint feed length and solder may affect the result.

Usage of the vector analyser allowed to obtain three results: – Resistance  $R$  (fig. 12a) – X-reactance (fig. 12b). As in the previous parameters case, also here we you can notice a dramatic deterioration of the results. From the value of  $53 \Omega$  of the simulated antenna, the result was  $30 \Omega$  higher. The operating bandwidth has been reduced by more than half compared to the simulated antenna. It is presented on the characteristics (Fig. 13.).The operating band is 149 MHz compared to required 75 MHz.

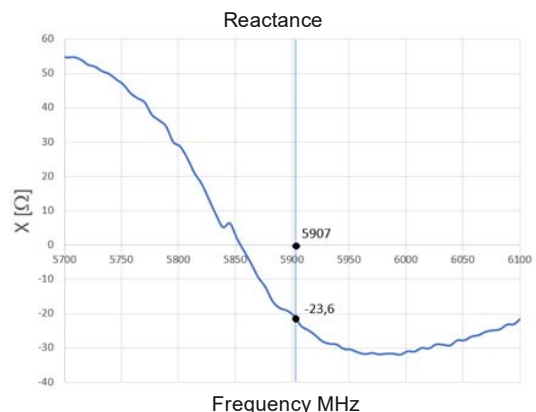
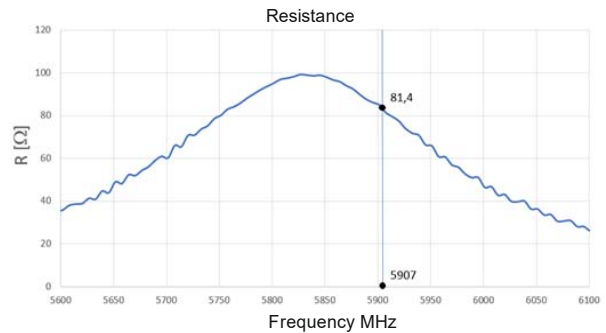


Fig. 12 Characteristics impedance of the made antenna

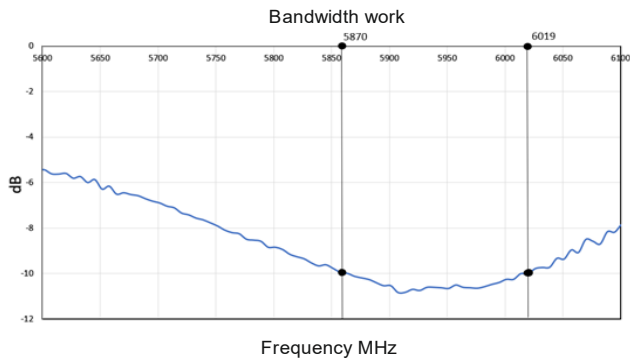


Fig. 13. Working band of the made antenna

These measurements were performed in an anechoic chamber which ensured adequate separation from external influences, and at the same time, the condition of the far zone was ensured [19].

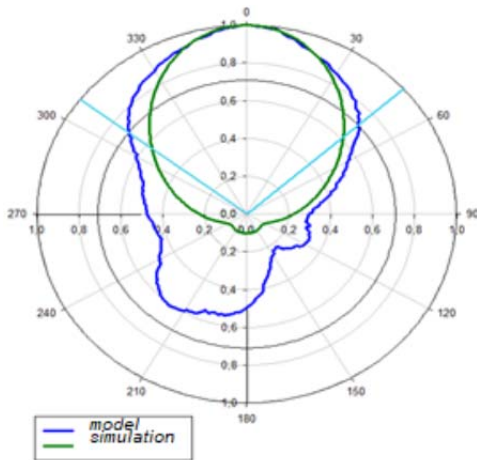


Fig. 14. The antenna radiation pattern for 5.9 GHz

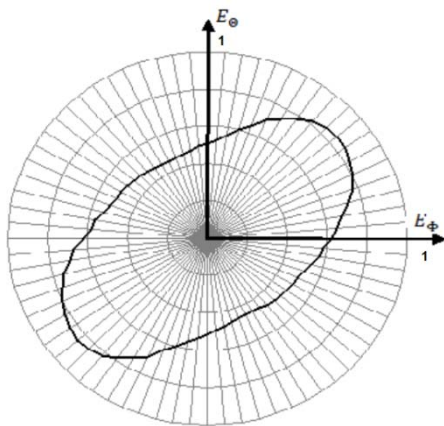


Fig. 15 Antenna polarization ellipse

The distortion of the back lobe may indicate an inaccurate representation (design) of the antenna. The designed antenna allows to receive signals in a wide range of angles  $95^\circ$ . As previously stated, the DSRC system - enables quick communication between vehicles and points on the roads or other vehicles while in motion. Thus, reflections may occur during the propagation of the electromagnetic wave. As a consequence it is difficult to predict the polarization of the wave reaching the receiver, and therefore it is difficult to properly select the polarization of the receiving antenna. This is important especially in the case of mobile devices. In their case, we you need to be

sure that they will work in any position. For this reason, sometimes loss of some power needs to be accepted or use two antennas with different polarities need to be used in the system. The situation of complete signal loss can then be prevented. The presented antenna has a rotating polarization and the elliptical coefficient is 5.46 dB. The polarization characteristics of the antenna is shown in Fig. 15.

### Conclusion

The article presents the concept and the physical model of an antenna for cooperation in the RFID system. The concept and design were created thanks to the review of antenna solutions in various technologies. The DSRC technology was characterized along with an indication of its advantages, examples of applications and the requirements of the IEEE 802.11p standard defining the standard of RFID systems operation. The developed antenna model is designed to work in the DSRC system. The values of electrical parameters and radiation characteristics obtained as a result of simulation were confirmed by measuring the physical model of the developed antenna. Both the obtained results of simulation and measurements confirm that the made antenna can work properly in the Dedicated Short-Range Communications system. In this via Toll system, i.e. the automatic toll collection system on European highways. The notches made in the sides of the antenna allowed to reduce the ellipticity of the characteristic, but at the same time worsened the input impedance. The performed model, in its operating band, is characterized by both capacitive and inductive reactance, which means that there is a great flexibility in choosing the RFID tag in order to create a coupled pair and maximize the power. The antenna made in the microstrip technology allowed to miniaturize its dimensions, therefore it is easy to install in portable radio communication devices. The obtained antenna radiation pattern has a width of  $95^\circ$ , thus ensuring the possibility of transmitting and receiving information in a large range of space. The bandwidth of the work is twice as large as the required requirements. These features and the obtained characteristics and parameters mentioned in the previous chapters put it at the forefront of currently developed solutions. The proposed antenna is an interesting alternative to other solutions of this type. Thanks to the rapid development of technology and the search for constant facilitation of our lives in all areas, the algorithms of the programs are constantly being improved, which allow for more and more accurate simulations of the tested elements.

### REFERENCES

- [1] Alibakhshi-Kenari M., Naser-Moghadasi M, Sadeghzadeh R A; "Composite Right-Left-Handed-Based Antenna with Wide Applications in Very-High Frequency-Ultra-High Frequency Bands for Radio Transceivers" *IET Microwaves, Antennas & Propagation*, Volume 9, Issue 15, 10 December 2015, p. 1713 – 1726.
- [2] Alibakhshi-Kenari M., Naser-Moghadasi M., Sadeghzadeh R.A.; "Bandwidth and Radiation Specifications Enhancement of Monopole Antennas Loaded with Split Ring Resonators" *IET Microwaves, Antennas & Propagation*, Volume 9, Issue 14, 19 November 2015, p. 1487 – 1496.
- [3] Alibakhshi-Kenari M., Naser-Moghadasi M.. "Novel UWB Miniaturized Integrated Antenna Based on CRLH Metamaterial Transmission Lines" *AEUE Elsevier- International Journal of Electronics and Communications*, Volume 69, Issue 8, August 2015, Pages 1143–1149
- [4] Morteza S. M.;Javad G. „Scannable Leaky-Wave Antenna Based on Ferrite-Blade Waveguide Operated below the Cutoff Frequency" *IEEE Transactions on Magnetics*, 2021, doi: 10.1109/TMAG.2021.3060683.

- [5] Huang J., „A Ka-Band Circularly Polarized High-Gain Microstrip Array Antenna” *IEEE Transactions on Antennas and Propagation* vol 43 Volume 1 1995
- [6] Karmakar N. C., “Handbook of smart antennas for RFID systems”, *Wiley*, 2010.
- [7] Akho-Zahieh M, Nasser A. “Performance Analysis of MIMO Wavelet Packet Multicarrier Multicode CDMA System with Antenna Selection” *Advances in Electrical and Electronic Engineering* 2019 vol. 17 iss: 4 pp 423-435 iss: 4 pp 423-435 ISSN 1804-3119. DOI: 10.15598/aeee.v17i4.3437
- [8] Z. Chudy, M. Wnuk: “Pomiar mocy impulsu elektromagnetycznego zakresu mikrofal” *Przegląd Elektrotechniczny* 2014 R. 90, nr 8 str: 239-242
- [9] Wnuk M. “Szerokopasmowa sonda pola elektromagnetycznego” *Przegląd Elektrotechniczny* 2021 R. 90, nr 10 str. 140 - 143
- [10] Narbudowicz A.Z., “Advanced Circularly Polarized Microstrip Patch Antennas”, *Dublin Institute of Technology*, 2013
- [11] Amanowicz M., Kołosowski W., Wnuk M. “Theoretical and experimental analysis of antennas on a dielectric substrate with rotating polarization”. *Department of Electronics, Military University of Technology in Warsaw* 2001.
- [12] Abhishek J, Singhal R, “Vertex-Fed Hexagonal Antenna with Low Cross-Polarization Levels” *Advances in Electrical and Electronic Engineering* 2019 vol. 17 iss: 2 pp 423-435 iss: 4 pp 138-145 ISSN 1804-3119 DOI: 10.15598/aeee.v17i2.3004
- [13] Fang, D. G. “Antenna theory and microstrip antennas”, *CRC Press* (2010)
- [14] Wnuk, M. “Analysis of radiating structures located on a multilayer dielectric” *Warsaw: MUT* (1999)
- [15] Taflove, A. “Computational electrodynamics Finite – Difference Time Domain”, *Artech House Boston* (1995).
- [16] Garg R., Bhartia P., Bahl I., Ittipiboon A., “Microstrip Antenna Design Book”, *Artech House* 2001
- [17] Yeo C. L., “Active Microstrip Array Antenna”, *The University of Queensland*, 2000
- [18] Sainati R. „CAD of Microstrip Antennas for Wireless Applications” *Artech House Boston London* 1996
- [19] Maloney, J. G., Smith, G. S. W. R., Scott, „Accurate computation of radiation from simple antennas using finite - difference time domain method”, *IEEE Trans. Antennas and Propagation* vol. 38 (1990),